Second-order nonlinear effects in asymmetric quantum-well structures

J. Khurgin*
Philips Laboratories, North American Philips Corporation, Briarcliff Manor, New York 10510
(Received 8 January 1988)

The expression for second-order optical susceptibility based on band-to-band and intraband transitions in various asymmetric multiple-quantum-well structures is derived. The analogy with organic nonlinear materials is shown. The dependence of the second-harmonic coefficient and Pockels coefficient on well geometry, band offsets, and other material parameters is studied. The nonlinear and electrooptic coefficients of GaAs-$Al_xGa_{1-x}As$ asymmetric quantum-well systems are estimated to be in the range of most conventional nonlinear materials, while for proposed ZnSe-GaAs heterostructures these coefficients are found to be substantially larger than in conventional materials. Some practical applications of asymmetric quantum-well systems are discussed, including novel methods of phase matching. The case for engineering of novel nonlinear materials is made.

I. INTRODUCTION

Recently there has been significant interest in nonlinear optical properties of quantum wells (QW's) and superlattices (SL's).[1,2] Calculations and observations of strong third-order nonlinearities were reported in GaAs-$Ga_{1-x}Al_xAs$ QW and SL structures. Among phenomena mentioned as leading to strong $\chi^{(3)}$ in such structures are conduction-band nonparabolicity,[3,4] exciton line saturation,[5] and the quantum confined Stark effect (QCSE).[6,7] Practical devices using QCSE, so-called self-electro-optic effect devices, have been successfully demonstrated.[8]

A typical multiple QW or SL system possesses an inversion symmetry; therefore, according to Ref. 9, only odd-order nonlinear effects can be observed. Second-order effects such as frequency mixing, including second-harmonic generation (SHG), and linear electrooptic effects are of great practical interest in the areas of integrated optics and optical communications. It is desirable to extend the frequency range of semiconductor lasers into the visible and to achieve tunability by means of frequency mixing and parametric amplification. Presently it is achieved using ordinary nonlinear materials, like $LiNbO_3$.[10] The efficiency of frequency conversion is poor primarily because it is hard to achieve high power density in the nonlinear crystal, due to low efficiency of coupling of highly divergent laser radiation into the nonlinear waveguide. Also there are considerable difficulties in growth and fabrication of nonlinear waveguides. On the other hand, power density inside the lasing layer approaches the order of MW/cm^2. The best way to achieve such high power density in the nonlinear material is, therefore, to grow it epitaxially on the same substrate as the lasing layer, thus creating truly integrated optical devices. Although large-band-gap III-V and II-VI materials which can be grown on GaAs or Si substrates possess second-order nonlinearity, they are cubic materials and phase matching is not easy.

Large third-order effects observed in QW structures suggest that once the inversion symmetry is removed, substantial second-order effects may result. Inversion symmetry and optical isotropy in the material can be destroyed by either applying an electric field externally or growing strained-layer,[11] doping,[12] or graded band-gap QW's and SL's with such a field built in. The electronic states of asymmetric QW's are similar to that of giant diatomic covalent molecules with various degrees of ionicity. Large dipole momentums of these "molecules" are lined up in the same direction of growth or applied field. According to Ref. 13, one should expect large nonlinear susceptibilities.

Such second-order nonlinearity based on virtual intraband transitions between the bound states in the conduction band of QW structures was first described in Ref. 14. The existence of such "envelope" transitions with large oscillator strength was recently confirmed by intraband absorption measurements of Levine *et al.*[15] A different approach to describing the nonlinear phenomena associated with electrons in the conduction band of the electrically biased SL's was suggested by Tsu and Esaki.[16] According to that approach, the nonlinearity results from nonparabolicity of conduction subbands in SL. Second-order effects mentioned in Refs. 14 and 16 are based on asymmetry of bound states or subbands separated from each other by energies less than conduction-band offset (about 0.1–0.3 eV for the $Ga_{1-x}Al_xAs$-GaAs heterostructure), so their use is limited by the free-carrier absorption to wavelengths larger than 5 μm.

A quasilinear shift in absorption spectra of asymmetric coupled QW's with applied electric field was recently observed and explained by Le *et al.*[17] and Little *et al.*[18] Nishi *et al.*[19] calculated linear QCSE in graded band-gap QW's. The effects described in Refs. 17–19 are the manifestation of the imaginary part of $\chi^{(2)}(\omega,0)$, although no explicit expressions were obtained for it in these papers.

In two recent papers, Yamanishi[20] and Chemla *et al.*[21] describe nonlinear processes associated with generation of virtual carriers in biased QW's by optical radiation with energy below absorption edge. The authors of Refs. 20 and 21 use a simple model based on interaction of virtual electrons and holes, but the effect can also be regard-

ed as optical rectification from the point of view of the standard nonlinear optics theory.[9]

In our recent work[22] an asymmetric coupled QW system was proposed as a medium with large real second-order susceptibility at the optical energies near band gap. Both SHG and Pockels coefficients were estimated to be comparable to most commonly used nonlinear and electrooptic materials.

In this work using Bloembergen's theory we derive the expression for second-order susceptibilities of asymmetric QW structures in Sec. II. The equivalency of that approach and virtual carriers approach used in Ref. 21 is shown. In Sec. III simplified formulas describing resonant SHG and Pockels effects are obtained. Section IV consists of the analysis of the second-order susceptibility for three possible implementations of such structures: asymmetric coupled QW's (ACQW's), linearly graded band-gap QW's (GBQW's), and biased QW's (BQW's). Three most important cases of second-order phenomena are examined: SHG, linear electrooptic effect, and optical rectification. The dependencies of these effects on the wide range of QW structure parameters are studied both by numerical calculations and by means of second-order perturbation theory calculations. The effect of absorption is determined. Finally, in Sec. V some practical applications are suggested, including methods of phase matching. Section VI contains conclusions.

II. DERIVATION OF THE $\chi^{(2)}$ EXPRESSION

The three asymmetric QW structures considered here are shown in Figs. 1(a) (GBQW), 1(b) (BQW), and 1(c) (ACQW). They are defined by the following set of parameters: d is the well thickness (in case of ACQW there are two well thicknesses $d_{1,2}$ and a barrier thickness t_b), B is the barrier thickness, ΔE_c is the maximum depth of the well in the conduction band, and ΔV is the potential drop across the well. Because we are interested in near-resonant susceptibility close to band-gap energy, only confined states are considered. The wave function of a bound state in the QW is

$$\Psi_{b,n}(k,r)=\phi_{b,n(r)}e^{ik_{\|}r_{\|}}=u_{b,n}(r)\psi_{b,n}(z)e^{ik_{\|}r_{\|}} , \tag{1}$$

where $u_{b,n}(r)$ is normalized Bloch's function of the band described by Kane,[23] $b=e$, lh, and hh for conduction, light-, and heavy-hole bands, respectively, $\psi_{b,n}(z)$ is a real normalized envelope wave function of the nth bound state, and $r_{\|}$ and $k_{\|}$ are the coordinate and wave vector in the xy plane.

The second-order susceptibility of such a multiple QW system can be calculated as[24]

$$\chi^{(2)}_{ijk}(\omega_1,\omega_2)=\frac{N_z e^3}{2\epsilon_0\hbar^2}\sum_P \sum_{b_1,b_2,b_3}\sum_{l,m,n} f_{b_1,l}\sum_{k_{\|}} \frac{\langle\phi^*_{1,l}\mid r_i\mid\phi_{2,m}\rangle\langle\phi^*_{2,m}\mid r_j\mid\phi_{3,n}\rangle\langle\phi^*_{3,n}\mid r_k\mid\phi_{1,l}\rangle}{[\omega_{b_2,m}(k_{\|})-\omega_{b_1,l}(k_{\|})-\omega_1-\omega_2][\omega_{b_3,n}(k_{\|})-\omega_{b_1,l}(k_{\|})-\omega_2]} , \tag{2}$$

where $\sum_P$ means summation over all terms obtained by permutation of the pairs $(-\omega_1-\omega_2,i)$, (ω_1,j), (ω_2,k), and $f_{b_1,l}$ is the Fermi function of the ground state $\phi_{1,l}$.

Because we are interested only in resonant effects and the lowest transition is that between ground electron state $e1$ and ground heavy-hole state hh1, we shall consider here only heavy-hole states. The light hole states' influence will be dealt with below. Also, in order to observe most interesting nonlinear effects, the light must propagate in the xy plane, so without loss of generality we assume it propagates in y direction. Consider now the product of three matrix elements in (2). If the light frequency is close to band gap, two of the states involved in the transitions must lie in one band and one state in the other band. Because Bloch's functions $u_{b,n}$ are orthonormal, the intraband matrix element in (2) is

$$\langle\phi^*_{b,m}\mid r_i\mid\phi_{b,n}\rangle=\langle\phi_{b,m}\mid z\mid\psi_{b,n}\rangle\delta_{i,z} . \tag{3}$$

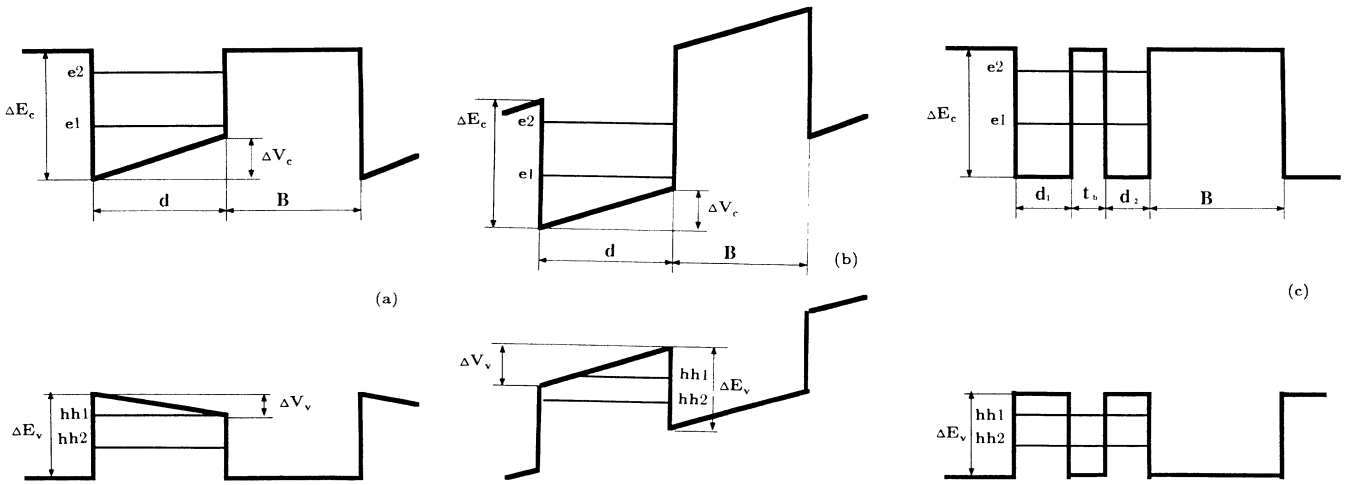

FIG. 1. Asymmetric multiple quantum well structures. (a) Graded band-gap quantum well. (b) Biased quantum well. (c) Asymmetric coupled quantum wells.

The interband matrix elements on the other hand are

$$\langle \phi^*_{e,m} \mid r_i \mid \phi_{\mathrm{hh},n} \rangle = \langle \psi_{e,m} \mid \psi_{\mathrm{hh},n} \rangle r_{e,\mathrm{hh}} \delta_{i,x} \ , \tag{4}$$

where $r_{e,\mathrm{hh}} = \langle u^*_e \mid u_{\mathrm{hh}} \rangle$ is interband matrix element of Bloch's functions, and $\delta_{i,z}$ follows from the fact that for heavy holes in QW structures $r_{e,\mathrm{hh}}$ is equal to 0 for the direction perpendicular to the QW plane.[25] Under all of the above assumptions, the only resonant contributions to $\chi^{(2)}$ are

$$\chi^2_{xzx}(\omega_1,\omega_2) = \frac{N_z e^3 r^2_{e,\mathrm{hh}}}{6\epsilon_0 \hbar^2} \sum_{k_\parallel} \sum_{m,n} \left[\sum_l \frac{\langle \psi_{\mathrm{hh}m} \mid \psi_{en} \rangle \langle \psi_{en} \mid z \mid \psi_{el} \rangle \langle \psi_{el} \mid \psi_{\mathrm{hh}m} \rangle}{[\omega^{en}_{\mathrm{hh}m}(k_\parallel) - \omega_1 - \omega_2][\omega^{el}_{\mathrm{hh}m}(k_\parallel) - \omega_1]} \right.$$
$$\left. - \frac{\langle \psi_{en} \mid \psi_{\mathrm{hh}m} \rangle \langle \psi_{\mathrm{hh}m} \mid z \mid \psi_{\mathrm{hh}l} \rangle \langle \psi_{\mathrm{hh}l} \mid \psi_{en} \rangle}{[\omega^{en}_{\mathrm{hh}m}(k_\parallel) - \omega_1 - \omega_2][\omega^{en}_{\mathrm{hh}l}(k_\parallel) - \omega_1]} \right] \tag{5a}$$

and

$$\chi^2_{zxx}(\omega_1,\omega_2) = \frac{N_z e^3 r^{(2)}_{e,\mathrm{hh}}}{6\epsilon_0 \hbar^2} \sum_{k_\parallel} \sum_{m,n} \left[\sum_l \frac{\langle \psi_{\mathrm{hh}m} \mid \psi_{en} \rangle \langle \psi_{en} \mid z \mid \psi_{el} \rangle \langle \psi_{el} \mid \psi_{\mathrm{hh}m} \rangle}{[\omega^{en}_{\mathrm{hh}m}(k_\parallel) - \omega_1][\omega^{el}_{\mathrm{hh}m}(k_\parallel) + \omega_2]} \right.$$
$$\left. - \frac{\langle \psi_{en} \mid \psi_{\mathrm{hh}m} \rangle \langle \psi_{\mathrm{hh}m} \mid z \mid \psi_{\mathrm{hh}l} \rangle \langle \psi_{\mathrm{hh}l} \mid \psi_{en} \rangle}{[\omega^{en}_{\mathrm{hh}m}(k_\parallel) - \omega_1][\omega^{en}_{\mathrm{hh}l}(k_\parallel) + \omega_2]} \right] , \tag{5b}$$

where the factor $\frac{1}{3}$ follows from averaging over polarization directions.

The positive term in the large parentheses represents sum of all the electrons susceptibilities and the negative sum of hole susceptibilities. From the point of view of Feinman's theory, the expression for electron (hole) susceptibility consists of the creation of a virtual carrier in the conduction (heavy-hole) band, its subsequent interaction with the electromagnetic field through intraband transitions and, finally, its annihilation. In the perturbation theory formalism, diagonal matrix elements of the intraband Hamiltonian in (5) represent a linear shift of the interband transition energy (linear quantum confined Stark effect) and nondiagonal elements represent linear changes in the oscillator strength of that transition. According to the oscillator sum rule these changes tend to cancel each other; therefore, one should expect that nonzero second-order susceptibility in QW structures must be a consequence of the difference in the nonresonant terms in the denominators in (5). Indeed, one can write for $l \neq n,m$

$$\frac{1}{\omega^{el}_{\mathrm{hh}m}(k_\parallel) - \omega_1} \approx \frac{1}{\omega^{en}_{\mathrm{hh}m}(k_\parallel) - \omega_1} - \frac{\omega^{en}_{el}(k_\parallel)}{[\omega^{en}_{\mathrm{hh}m}(k_\parallel) - \omega_1]^2} \tag{6a}$$

and

$$\frac{1}{\omega^{en}_{\mathrm{hh}l}(k_\parallel) - \omega_1} \approx \frac{1}{\omega^{en}_{\mathrm{hh}m}(k_\parallel) - \omega_1} - \frac{\omega^{\mathrm{hh}m}_{\mathrm{hh}l}(k_\parallel)}{[\omega^{en}_{\mathrm{hh}m}(k_\parallel) - \omega_1]^2} \ . \tag{6b}$$

Because we are interested in $\chi^{(2)}$ near the band gap, only the terms with low m,n indices are significant. For small m,n overlap integrals with rapidly oscillating unconfined levels can be neglected, and then one can assume that $\psi_{\mathrm{hh}l}$ and ψ_{el} are complete sets of orthonormal wave functions. Substituting (6) into (5a) one obtains

$$\chi^{(2)}_{xzx}(\omega_1,\omega_2) = -\frac{N_z e^3 r^2_{e,\mathrm{hh}}}{6\epsilon_0 \hbar^2} \sum_{k_\parallel} \sum_{m,n} \frac{\langle \psi_{en} \mid \psi_{\mathrm{hh}m} \rangle}{[\omega^{en}_{\mathrm{hh}m}(k_\parallel) - \omega_1 - \omega_2][\omega^{en}_{\mathrm{hh}m}(k_\parallel) - \omega_1]^2}$$
$$\times \left[\sum_{l\ (\neq n)} \langle \psi_{en} \mid z \mid \psi_{el} \rangle \langle \psi_{el} \mid \psi_{\mathrm{hh}m} \rangle \omega^{en}_{el}(k_\parallel) \right.$$
$$\left. - \sum_{l\ (\neq m)} \langle \psi_{\mathrm{hh}m} \mid z \mid \psi_{\mathrm{hh}l} \rangle \langle \psi_{\mathrm{hh}l} \mid \psi_{en} \rangle \omega^{\mathrm{hh}m}_{\mathrm{hh}l}(k_\parallel) \right] . \tag{7}$$

Because the right-hand side of Eq. (5b) does not have resonance at $\omega = \omega_1 + \omega_2$, $\chi^{(2)}_{zxx}$ is much smaller than χ_{xzx} and we shall not consider it till later in the paper. Further simplification is achieved by going from summation over the k vector to integration over energy, introducing line broadening Γ, and assuming that the following effective mass approximation energy splits between sublevels within one band are independent of the wave vector:

$$\omega^{en}_{el}(k_\parallel) = \omega^{el}_{en} \ , \tag{8a}$$

$$\omega^{\mathrm{hh}m}_{\mathrm{hh}l}(k_\parallel) = \omega^{\mathrm{hh}m}_{\mathrm{hh}l} \ . \tag{8b}$$

Performing integration one obtains

$$\chi^{(2)}_{xzx}(\omega_1,\omega_2) = \frac{m_r e r^2_{e,\mathrm{hh}}}{3a_0(E_{\mathrm{gap}} - \hbar\omega_1)} \left[\sum_{m,n,l>n} \chi^{(2),e}_{m,n,l} - \sum_{m,n,l>m} \chi^{(2),h}_{m,n,l} \right] , \tag{9}$$

where $E_{\rm gap}$ is the average band gap of the bulk material, m_r is reduced effective mass in units of m_0, $m_r^{-1}=m_e^{-1}+m_{\rm hh}^{-1}$, a_0 is Bohr's radius, and dimensionless nonlinear susceptibilities are

$$\chi^{(2),e}_{m,n,l}=-N_z\langle\psi_{{\rm hh}m}\mid\psi_{en}\rangle\langle\psi_{en}\mid z\mid\psi_{el}\rangle\langle\psi_{el}\mid\psi_{{\rm hh}m}\rangle\frac{\omega^{en}_{el}}{\omega^{en}_{{\rm hh}m}-\omega_1}\ln\frac{(\hbar\omega^{en}_{el}+\delta_{n,m})^2+\Gamma^2}{\delta^2_{n,m}+\Gamma^2} \tag{10a}$$

for electrons and

$$\chi^{(2),{\rm hh}}_{m,n,l}=-N_z\langle\psi_{en}\mid\psi_{{\rm hh}m}\rangle\langle\psi_{{\rm hh}m}\mid z\mid\psi_{{\rm hh}l}\rangle\langle\psi_{{\rm hh}l}\mid\psi_{em}\rangle\frac{\omega^{{\rm hh}m}_{{\rm hh}l}}{\omega^{en}_{{\rm hh}m}-\omega_1}\ln\frac{(\hbar\omega^{{\rm hh}m}_{{\rm hh}l}+\delta_{n,m})^2+\Gamma^2}{\delta^2_{n,m}+\Gamma^2} \tag{10b}$$

for heavy holes, where $\delta_{n,m}=\hbar\omega^{en}_{{\rm hh}m}-\hbar\omega_1-\hbar\omega_2$ is detuning.

In order to better estimate magnitude of the $\chi^{(2)}$ and compare it with linear susceptibility of the bulk material, one can write

$$\chi^{(2)}_{xzx}(\omega_1,\omega_2)=(\epsilon_r-1)\frac{m_r a^3\epsilon_0}{a_0 e}\frac{\bar{E}_{\rm gap}}{E_{\rm gap}-\hbar\omega_1}\chi^{(2)}(\delta)\ , \tag{11}$$

where ϵ_r is the long-wavelength dielectric constant of bulk material, $\bar{E}_{\rm gap}$ is the mean gap energy, used by Penn,[26] usually a few times larger than $E_{\rm gap}$, a is the lattice constant, and $\chi^{(2)}$ denotes the sum of all dimensionless nonlinear susceptibilities in the large parentheses of (9). If one uses GaAs as a benchmark material, then for a large class of III-V and II-VI materials (11) can be rewritten as

$$\chi^2_{xzx}(\omega_1,\omega_2)\approx AF\chi^{(2)}(\delta)\ , \tag{12}$$

where $A=0.96\times10^{-10}$ m/V, and

$$F=\frac{m_r}{m_{r,{\rm GaAs}}}\frac{E_{\rm gap,GaAs}}{E_{\rm gap}-\hbar\omega_1}\ . \tag{13}$$

As one can see, the expression for nonlinear susceptibility is now separated into two factors: One of them, F, is material dependent through the effective masses and band gap, and the other one, $-\chi^{(2)}$, which is dependent on the shape of the QW's. The nonlinear susceptibility seems to increase with increase in m_r because the number of confined states increases. However, $\chi^{(2)}$ also depends on effective mass in a more complicated way which needs to be studied.

III. $\chi^{(2)}$ DEPENDENCE ON QW PARAMETERS

Let us now further simplify our task by assuming that only two confined levels in each band contribute to nonlinear susceptibility. Assuming completeness of the set of envelope functions, one obtains

$$\chi^{(2)}(\delta)=[\chi^{(2)}_{\rm hh}f_{\rm hh}(\delta)-\chi^{(2)}_e f_e(\delta)]\ , \tag{14a}$$

where the geometrical electron susceptibility is

$$\chi^{(2)}_e=N_z\langle\psi_{h1}\mid\psi_{e1}\rangle\langle\psi_{e1}\mid z\mid\psi_{e2}\rangle\langle\psi_{e2}\mid\psi_{h1}\rangle\ , \tag{14b}$$

geometrical hole susceptibility is

$$\chi^{(2)}_{\rm hh}=N_z\langle\psi_{e1}\mid\psi_{h1}\rangle\langle\psi_{h1}\mid z\mid\psi_{h2}\rangle\langle\psi_{h2}\mid\psi_{e1}\rangle\ , \tag{14c}$$

and band-splitting factors are

$$f_{\rm hh}(\delta)=\frac{\hbar\omega^{\rm hh2}_{\rm hh1}}{\hbar\omega^{e1}_{\rm hh2}-\hbar\omega_1}\ln\frac{(\hbar\omega^{\rm hh2}_{\rm hh1}+\delta)^2+\Gamma^2}{\delta^2+\Gamma^2}-\frac{\hbar\omega^{\rm hh2}_{\rm hh1}}{\hbar\omega^{e2}_{\rm hh2}-\hbar\omega_1}\ln\frac{(\hbar\omega^{\rm hh2}_{\rm hh1}+\hbar\omega^{e2}_{e1}+\delta)^2+\Gamma^2}{(\delta+\hbar\omega^{e2}_{e1})^2+\Gamma^2} \tag{15a}$$

for holes and

$$f_e(\delta)=\frac{\hbar\omega^{e2}_{e1}}{\hbar\omega^{e2}_{\rm hh1}-\hbar\omega_1}\ln\frac{(\hbar\omega^{e2}_{e1}+\delta)^2+\Gamma^2}{\delta^2+\Gamma^2}-\frac{\hbar\omega^{e2}_{e1}}{\hbar\omega^{e2}_{\rm hh2}-\hbar\omega_1}\ln\frac{(\hbar\omega^{e2}_{e1}+\hbar\omega^{\rm hh2}_{\rm hh1}+\delta)^2+\Gamma^2}{(\delta+\hbar\omega^{\rm hh2}_{\rm hh1})^2+\Gamma^2} \tag{15b}$$

for electrons. In the above expressions, splitting factors in the first order depend only on band offsets, effective masses, and the well width, while geometrical susceptibilities depend mostly on the degree of asymmetry of the wells.

We shall now consider three distinct situations: SHG, linear electrooptics effect, and optical rectification. These situations differ primarily by the fact that the denominator in first term of the splitting factors in the last two cases can become quite small for small detuning δ, while for the SHG coefficient that term is practically independent of detuning. The dimensionless second harmonic coefficient $D^{(2\omega)}$ has only one resonant component:

$$D^{(2\omega)}_{15}(\delta)=[\chi^{(2)}_{\rm hh}f^{2\omega}_{\rm hh}(\delta)-\chi^{(2)}_e f^{2\omega}_{ee}(\delta)]\ , \tag{16}$$

where band-splitting factors are

$$f^{2\omega}_{\rm hh}(\delta)\approx\frac{2\hbar\omega^{\rm hh2}_{\rm hh1}}{E_{\rm gap}}\left[\ln\frac{(\hbar\omega^{\rm hh2}_{\rm hh1}+\delta)^2+\Gamma^2}{\delta^2+\Gamma^2}-\ln\frac{(\hbar\omega^{\rm hh2}_{\rm hh1}+\hbar\omega^{e2}_{e1}+\delta)^2+\Gamma^2}{(\delta+\hbar\omega^{e2}_{e1})^2+\Gamma^2}\right] \tag{17a}$$

and

$$f^{2\omega}_e(\delta)\approx\frac{2\hbar\omega^{e2}_{e1}}{E_{\rm gap}}\left[\ln\frac{(\hbar\omega^{e2}_{e1}+\delta)^2+\Gamma^2}{\delta^2+\Gamma^2}-\ln\frac{(\hbar\omega^{e2}_{e1}+\hbar\omega^{\rm hh2}_{\rm hh1}+\delta)^2+\Gamma^2}{(\delta+\hbar\omega^{\rm hh2}_{\rm hh1})^2+\Gamma^2}\right]\ , \tag{17b}$$

and where $\delta=\hbar\omega_{hh1}^{e1}-2\omega$, and relation between real and dimensionless SHG coefficients is

$$d_{15}^{(2\omega)}=AF^{(2\omega)}D_{15}^{(2\omega)}(\delta)\ , \tag{18a}$$

where

$$F^{(2\omega)}=2\frac{m_r}{m_{r,\mathrm{GaAs}}}\frac{E_{g,\mathrm{GaAs}}}{E_g}\ . \tag{18b}$$

For linear electrooptics effect, one obtains

$$R_{13}(\delta)=[\chi_{hh}^{(2)}f_{hh}^{(0)}(\delta)-\chi_e^{(2)}f_{ee}^{0}(\delta)]\ , \tag{19}$$

where band-splitting factors are

$$f_{hh}^{0}(\delta)\approx\ln\frac{(\hbar\omega_{hh1}^{hh2}+\delta)^2+\Gamma^2}{\delta^2+\Gamma^2} \tag{20a}$$

and

$$f_e^{0}(\delta)\approx\ln\frac{(\hbar\omega_{e1}^{e2}+\delta)^2+\Gamma^2}{\delta^2+\Gamma^2}\ , \tag{20b}$$

and where $\delta=\hbar\omega_{hh1}^{e1}-\omega$ and relation between real and dimensionless Pockels coefficients is

$$\tfrac{1}{2}n^4r_{13}^{\omega}=AF^{(\omega)}R_{13}(\delta)\ , \tag{21a}$$

where

$$F^{(\omega)}=\frac{m_r}{m_{r,\mathrm{GaAs}}}\frac{E_{g,\mathrm{GaAs}}}{h\delta}\ . \tag{21b}$$

There is also a much smaller Pockels coefficient R_{51} coming from Eq. (5b), where both x- and z-polarized light are involved in the virtual transitions but only the x-polarized component is close to resonant with interband transitions:

$$R_{51}(\delta)=[\chi_{hh}^{(2)}f_{hh}^{51}(\delta)-\chi_e^{(2)}f_{ee}^{51}(\delta)]\ , \tag{22}$$

where band-splitting factors are

$$f_{hh}^{51}(\delta)\approx\tfrac{1}{2}f_{hh}^{2\omega}(\delta) \tag{23}$$

and

$$f_e^{51}(\delta)\approx\tfrac{1}{2}f_e^{2\omega}\ , \tag{24}$$

and relation between real and dimensionless Pockels coefficients is

$$\tfrac{1}{2}n^4r_{51}^{\omega}=AF_{51}^{(\omega)}R_{51}(\delta)\ , \tag{25a}$$

where

$$F_{51}^{(\omega)}=\frac{m_r}{m_{r,\mathrm{GaAs}}}\frac{E_{g,\mathrm{GaAs}}}{E_g}\ . \tag{25b}$$

Although much smaller than r_{13}^{ω}, the coefficient r_{51} can lead to many interesting phenomena in the waveguide geometry involving nonlinear interaction of TE and TM modes, but that subject is beyond the scope of the present paper, and we shall consider only the "double-resonant" Pockels coefficient r_{31} from now on.

Finally, the optical rectification coefficient in accordance with the Kleinman rule is equal to the Pockels coefficient

$$S_{31}(\delta)=R_{13}(\delta)\ . \tag{26}$$

IV. RESULTS AND DISCUSSION

The results of calculations for the dimensionless SHG coefficient and for the Pockels coefficient are shown in Figs. 2–4 for GBQW, BQW, and ACQW, respectively. The barrier in all examples is made of $Ga_{0.4}Al_{0.6}As$, and the well in all examples is either pure GaAs or, in the case of GBQW, is graded from GaAs to $Ga_{1-x}Al_xAs$ where $x<0.6$. The maximum conduction band offset ΔE_c is thus 300 meV and, corresponding to it, the valence band offset is 200 meV. Detuning δ in all cases was assumed to be 75 meV, which in material of good quality should eliminate absorption. The existence of Urbach's tail may, of course, interfere and lead to increased absorption, but we shall neglect it for now.

In Figs. 2(a) and 2(b) the dependence of $D_{15}^{(2\omega)}(\delta)$ and $R_{13}^{(\omega)}(\delta)$ on the tilt of the conduction band of GBQW, ΔV_c, are shown for different thicknesses of wells. Both second-harmonic and electrooptical coefficient first rapid-

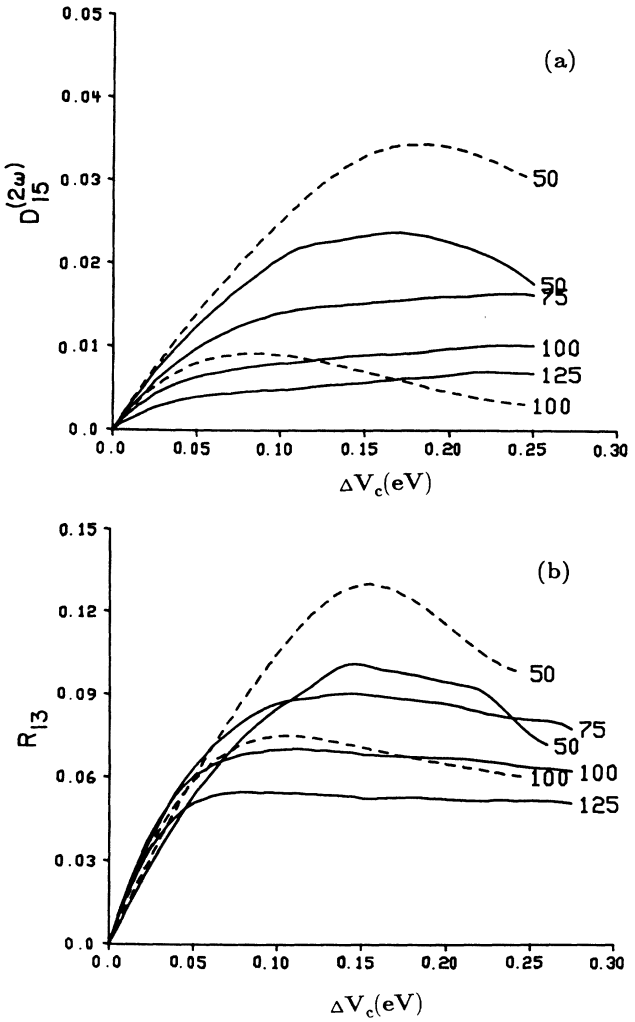

FIG. 2. Dimensionless SHG coefficient $D_{15}^{(2\omega)}$ (a) and Pockels coefficient R_{13} (b) of GaAs-$Al_{0.4}Ga_{0.6}As$ GBQW as functions of potential gradient across the well in the conduction band ΔV_c for various well thicknesses d. Solid lines: exact wave-function calculations. Dashed lines: first-order perturbation calculations.

ly increase with an increase in tilt, and then either saturate or even decrease. This behavior can be explained by the fact that small increase in tilt or, in other words, in well asymmetry, causes previously prohibited transitions in Eq. (14) to become partially allowed, thus increasing $\chi^{(2)}$, while large tilts cause a decrease in oscillator strength of nominally allowed transition in Eq. (14) and thus a decrease in $\chi^{(2)}$.

Both $d_{15}^{(2\omega)}(\delta)$ and $R_{13}^{(\omega)}(\delta)$ are larger for thinner wells. This behavior is caused by larger energy splits $\hbar\omega_{hh1}^{hh2}$ and $\hbar\omega_{e1}^{e2}$ reducing the cancellation due to contributions of states with opposite polarity. Unfortunately, in very thin wells, level $e2$ becomes unconfined and such states are not considered in this paper, although they can also contribute to nonlinearity of the superlattice.

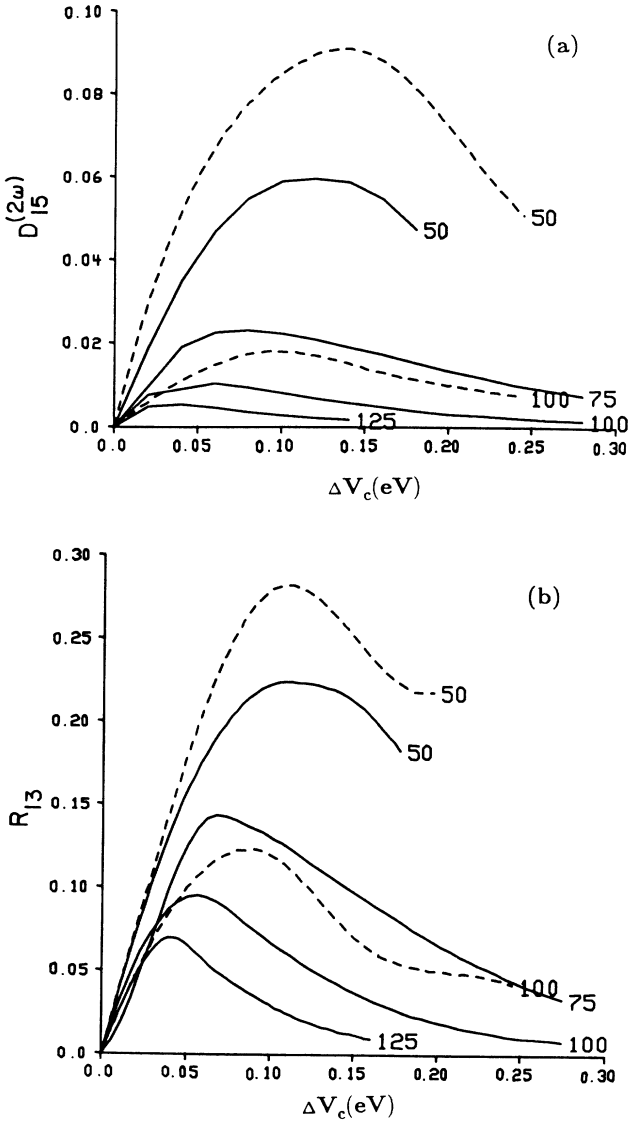

FIG. 3. Dimensionless SHG coefficient $D_{15}^{(2\omega)}$ (a) and Pockels coefficient R_{13} (b) of GaAs-$Al_{0.4}Ga_{0.6}As$ BQW as functions of potential drop across the well in the conduction band ΔV_c for various well thicknesses d. Solid lines: exact wave-function calculations. Dashed lines: first-order perturbation calculations.

In absolute values, $D_{15}^{(2\omega)}(\delta)$ reaches a maximum of 0.025 corresponding, according to Eq. (18), to $d_{15}^{(2\omega)} \approx 5\times10^{-12}$ m/V. That value is comparable to values for $LiNbO_3$ or $KTiOPO_4$. For the linear electro-optic coefficient $R_{13}^{(\omega)}(\delta)$ the maximum value is 0.1 and, therefore, according to (21), $r_{13}^{\omega} \approx 3.1\times10^{-12}$ m/V, and the practical value is $n^3 r_{13}^{\omega} \approx 1.1^{-10}$ m/V, which is better than for bulk GaAs.

In Figs. 3(a) and 3(b) the dependencies of $D_{15}^{(2\omega)}(\delta)$ and $R_{13}^{(\omega)}(\delta)$ on the tilt of the conduction band of BQW, ΔV_c, are shown for different thicknesses of wells. Both second harmonic and electrooptical coefficients are somewhat larger than in the case of GBQW, and their thickness and band tilt dependencies are similar to the GBQW case, except the curves tend to saturate faster, which follows from the fact that the $e2$ function becomes unconfined by tunneling from the well. The increase of nonlinearity of

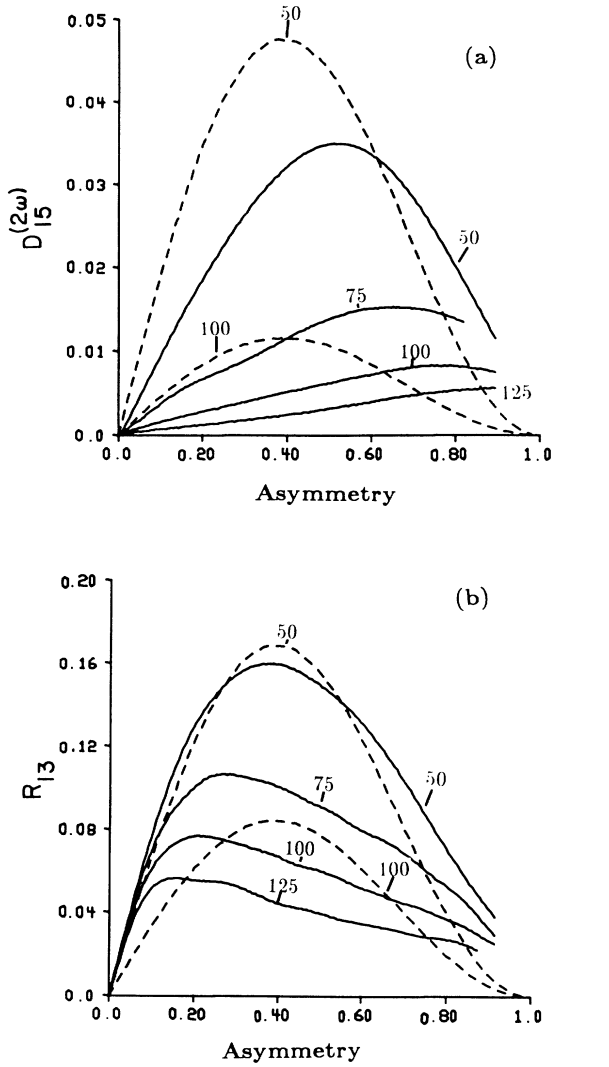

FIG. 4. Dimensionless SHG coefficient $D_{15}^{(2\omega)}$ (a) and Pockels coefficient R_{13} (b) of GaAs-$Al_{0.4}Ga_{0.6}As$ ASQW as functions of well asymmetry s for various total well thicknesses d_1+d_2 and constant barrier thickness $t_b = 10$ Å. Solid lines: exact wave-function calculations. Dashed lines: first-order perturbation calculations.

the BQW can be easily explained by the fact that virtual holes and electrons in the BQW are moved in opposite directions by the band-gap gradient, while in the GBQW they move in the same direction; thus nonlinear dipole momentum is larger in the BQW. In the $Ga_{1-x}Al_xAs$ BQW the maximum dimensionless SHG coefficient $D_{15}^{(2\omega)}(\delta)=6\times10^{-2}$, corresponding to $d_{15}^{(2\omega)}\approx1.2\times10^{-11}$ m/V. For the BQW electrooptical coefficient the maximum value of $R_{13}^{(\omega)}(\delta)$ is 0.23, corresponding to $r_{13}^{\omega}=\approx7.1\times10^{-12}$ m/V, and $n^3r_{13}^{\omega}\approx2.3^{-10}$ m/V, a value only 1.5 times smaller than $LiNbO_3$.

For the ACQW, besides total thickness d, second-order susceptibility depends on two parameters (Fig. 1): barrier thickness t_b and asymmetry parameter $s=(d_1-d_2)/(d_1+d_2)$. If we consider the "diatomic molecular analogy," s can be loosely treated as ionicity and t_b as binding energy. In Figs. 4(a) and 4(b) the dependence of $D_{15}^{(2\omega)}(\delta)$ and $R_{13}^{(\omega)}(\delta)$ on the degree of asymmetry is shown for different thicknesses of wells for fixed $t_b=10$ Å. Both second-harmonic and electrooptical coefficients exhibit similar dependence on asymmetry. The interesting point is that both have their maximums close to $s=0.5$ which qualitatively agrees with most theoretical investigations of nonlinearity, where the diatomic materials where shown to have maximum $\chi^{(2)}$ when their bonds are somewhere in between purely ionic and purely covalent.

In Figs. 5(a) and 5(b) the dependencies of $D_{15}^{(2\omega)}(\delta)$ and $R_{13}^{(\omega)}(\delta)$ on the barrier thickness t_b for different s are shown. The overall well thickness is kept at 50 Å. 10 Å seems to be about the optimal barrier thickness for both SHG and Pockels coefficients.

In the $Ga_{1-x}Al_xAs$ ASQW the maximum dimensionless SHG coefficient $D_{15}^{(2\omega)}(\delta)\approx4\times10^{-2}$, corresponding to $d_{15}^{(2\omega)}\approx6\times10^{-12}$ m/V. For the ASQW electrooptical coefficient the maximum value of $R_{13}^{(\omega)}(\delta)$ is 0.15, corresponding to $r_{13}^{\omega}\approx4.9\times10^{-12}$ m/V, and $n^3r_{13}^{\omega}\approx1.8^{-10}$ m/V.

Comparing the three geometries one concludes that the BQW has the largest values of nonlinear coefficients, but it also is the least practical of geometries, requiring either external fields or large stress. Therefore, for practical applications the ACQW seems to be the most appropriate candidate. Some additional improvement in $\chi^{(2)}$ can be achieved by combining the ACQW and GBQW.

In order to more deeply understand the influence of material parameters on $\chi^{(2)}$ it is desirable to obtain an analytical expression for $\chi^{(2)}$ which does not require calculation of wave functions. One can obtain a simple rough approximation for $D_{15}^{(2\omega)}(\delta)$ and $R_{13}^{(\omega)}(\delta)$ of the GBQW and BQW by treating asymmetry as a small perturbation to the infinitely deep square QW and assuming that energy splits $\hbar\omega_{e1}^{e2}$ and $\hbar\omega_{hh1}^{hh2}$ are much smaller than the band gap:

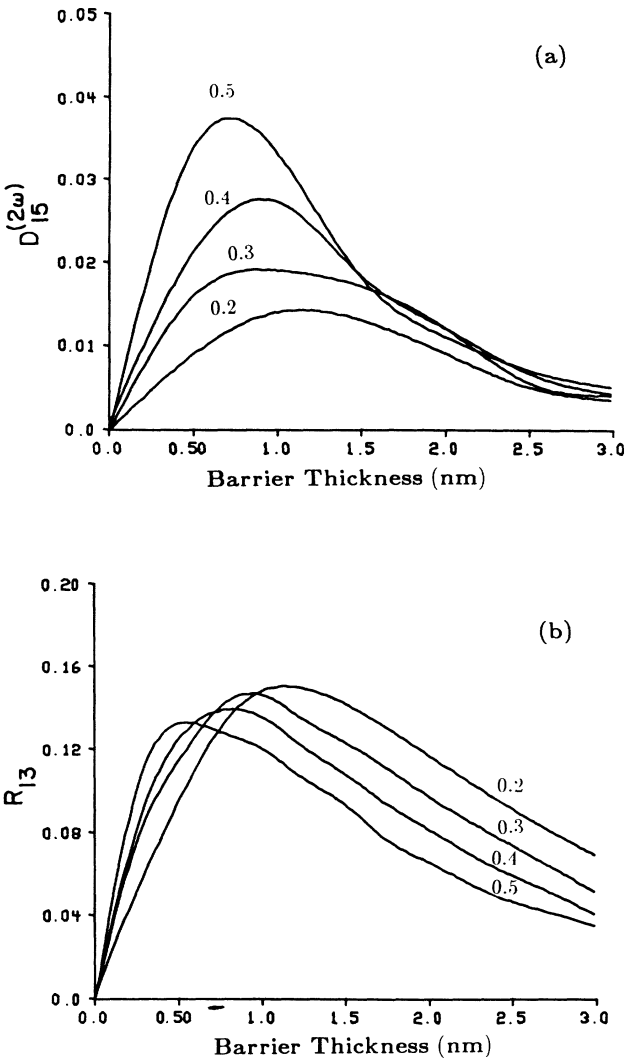

FIG. 5. Dimensionless SHG coefficient $D_{15}^{(2\omega)}$ (a) and Pockels coefficient R_{13} (b) of GaAs-$Al_{0.4}Ga_{0.6}As$ ASQW as functions of barrier thickness t_b for various well asymmetries s and constant total well thickness $d_1+d_2=50$ Å.

$$D_{15}^{(2\omega)}(\delta)\approx\frac{C^{(2\omega)}}{d^4}(\theta_e m_e^{-1}+\theta_{hh}m_{hh}^{-1})\times\frac{(\theta_e m_e^{-1}\Delta V_v-\theta_{hh}m_{hh}^{-1}\Delta V_c)}{\hbar(\omega_{hh1}^{e1}-\omega_1)\delta^2}S(d) \quad (27)$$

and

$$R_{13}^{(\omega)}(\delta)\approx C^{(\omega)}(\theta_e m_e^{-1}+\theta_{hh}m_{hh}^{-1})\times\frac{(m_e\theta_e^{-1}\Delta V_v-m_{hh}\theta_{hh}^{-1}\Delta V_c)}{\delta}S(d)\,, \quad (28)$$

where

$$S(d)=\frac{1+K^2m_e\Delta V_c\theta_e^{-1}m_v\theta_{hh}^{-1}\Delta V_v d^4}{[1+(Km_e\theta_e^{-1}d^2\Delta V_c)^2]^2[1+(K_v m_{hh}\theta_{hh}^{-1}d^2\Delta V_v)^2]^2} \quad (29)$$

is a correction factor arising from the reduction of the oscillator strength of the allowed transitions in the tilted well:

$$C^{(2\omega)}=\frac{4}{9}\frac{h^2}{m_0}=0.7\times 10^2\ \text{eV}^2\,\text{Å}^4\ , \tag{30a}$$

$$C^{(\omega)}=0.04\ , \tag{30b}$$

$$K=\frac{16}{9\pi^2}\frac{2m_0}{3\pi^2\hbar^2}=0.17\ \text{eV}^{-1}\,\text{Å}^{-2}\ ; \tag{31}$$

$$\theta_e=\frac{\hbar\omega_{e1}^{e2}(\Delta E_c)}{\hbar\omega_{e1}^{e2}(\infty)}$$

$$\approx 1-\frac{2}{1+0.71\pi(\gamma\Delta E_c m_e d^2-1)^{1/2}} \tag{32a}$$

and

$$\theta_{\text{hh}}=\frac{\hbar\omega_{\text{hh1}}^{\text{hh2}}(\Delta E_v)}{\hbar\omega_{\text{hh1}}^{\text{hh2}}(\infty)}$$

$$\approx 1-\frac{2}{1+0.71\pi(\gamma\Delta E_c m_{\text{hh}} d^2-1)^{1/2}} \tag{32b}$$

are ratios of the energy splits between the lowest confined states of the real wells and the energy splits in the case of infinite depth wells, for conduction and heavy-hole bands, respectively, where ΔE_c and ΔE_v are band offsets and

$$\gamma=\frac{2m_0}{\pi^2\hbar^2}=0.029\ \text{eV}^{-1}\,\text{Å}^{-2}\ . \tag{33}$$

For the ACQW perturbation theory assuming very thin barriers yields the following results:

$$D_{15}^{(2\omega)}(\delta)\approx\frac{C_{\text{ACQW}}^{(2\omega)}}{d^4}\frac{t_b}{d}(\theta_e m_e^{-1}+\theta_{\text{hh}}m_{\text{hh}}^{-1})\times\frac{(\theta_e m_e^{-1}\Delta E_v-\theta_{\text{hh}}m_{\text{hh}}^{-1}\Delta E_c)}{\hbar(\omega_{\text{hh1}}^{e1}-\omega_1)\delta^2}\times\cos\left[\frac{\pi s}{2}\right]\sin(\pi s)S(d) \tag{34}$$

and

$$R_{13}^{(\omega)}(\delta)\approx C_{\text{ACQW}}^{(\omega)}\frac{t_b}{d}(\theta_e m_e^{-1}+\theta_{\text{hh}}m_{\text{hh}}^{-1})\times\frac{(m_e\theta_e^{-1}\Delta E_v-m_{\text{hh}}\theta_{\text{hh}}^{-1}\Delta E_c)}{\delta}\times\cos\left[\frac{\pi s}{2}\right]\sin(\pi s)S(d)\ , \tag{35}$$

where

$$C_{\text{ACQW}}^{(2\omega)}=\frac{\pi^2}{4}\frac{h^2}{m_0}=3.8\times 10^2\ \text{eV}^2\,\text{Å}^4\ , \tag{36a}$$

$$C_{\text{ACQW}}^{(\omega)}=0.22\ . \tag{36b}$$

The results of the approximate analysis are plotted in Figs. 2–4 as dashed lines. The approximate expressions (27) and (28) fail to predict correct values of $D_{15}^{(2\omega)}(\delta)$ and $R_{13}^{(\omega)}(\delta)$, especially for large asymmetries, due to the fact that the influence of asymmetry on level splitting is not included in (27) and (28) and penetration of the wave function into the barrier is discounted. Also, by linearizing logarithmic expressions in (15), the dependence on d is overestimated. Still, qualitatively, expressions (27) and (28) are correct and allow us to make general observations about nonlinear susceptibilities of asymmetric QW's.

First, it is very clear that nonlinear susceptibility in the BQW is always larger than in the GBQW because for the BQW the band tilts are of opposite sign, $\Delta V_v=-\Delta V_c$, while for the GBQ they are of the same sign, $\Delta V_v=\Delta V_c\Delta E_v/\Delta E_c$. It also follows that for light holes the nonlinear susceptibility of the $Ga_{1-x}Al_xAs$ GBQW or ASQW is very small because the term in parentheses in (27) and (28) and (34) and (35) is almost exactly zero, due to

$$\frac{m_{\text{lh}}}{m_e}\approx\frac{\Delta E_c}{\Delta E_v}=1.4\ . \tag{37}$$

These results were also obtained by the authors of Ref. 24 in their calculation of the QCSE in the GBQW. The absence of nonlinear susceptibility $\chi_{33}^{(2)}$ is, therefore, just a peculiar feature of the GaAs-$Ga_{1-x}Al_xAs$ system, and in materials made of other material one can obtain significant $d_{33}^{(2\omega)}$ and $r_{33}(\omega)$, of which the first one is of major importance as one allowing type-I phase matching.

The most important is, of course, the dependence of nonlinear constants on the size of the well. The dependence of $D_{15}^{(2\omega)}(\delta)$ on d is very strong, due to "triple" cancelation described in Sec. II, which occurs when levels become very close to each other. One then should try to keep the wells as small as possible, yet then levels become less confined and less asymmetrical. The dependence on effective masses is even more complex because on one hand smaller effective mass increases level energy splits, but on the other hand it leads to reduced density of states, thus reducing the number of states creating nonlinear polarization via the term m_r in (11).

From the point of view of material engineering it would be most interesting to obtain the dependence of $\chi^{(2)}$ on band offsets and effective masses. Assuming that

$$\frac{m_{\text{hh}}}{m_e}=r_m>r_e=\frac{\Delta E_c}{\Delta E_v}\ , \tag{38}$$

one obtains

$$d_{15}^{(2\omega)}\sim m_r\Delta E_c^3 r_m^{-1}\left[\frac{r_m}{r_e}\pm 1\right](r_m^{-1}+1) \tag{39}$$

and

$$r_{13}^{(\omega)}\sim m_r\Delta E_c\left[\frac{r_m}{r_e}\pm 1\right](r_m^{-1}+1)\ , \tag{40}$$

where the + sign in the large parentheses corresponds to the BQW and − to the GBQW and ACQW.

According to (39) and (40) one has to look for materials with large band discontinuities and large effective masses,

though the difference between effective masses of conduction and valence bands should be large. Unfortunately, for many interesting combinations of materials, the band offsets are not known. As an example of a system with large band offsets, one may consider the GaAs-ZnSe lattice-matched heterostructure. Although no structure like that has ever been grown yet, we find it is still interesting to see what kind of nonlinearities one may expect in such systems. The band-gap offsets are $\Delta E_v \approx 960$ meV and $\Delta E_c \approx 300$ meV.[27] We have chosen the ACQW as an example. The largest SHG coefficient was obtained for two coupled QW's of $d_1 = 25$ Å and $d_2 = 12$ Å separated by a 5-Å barrier, $d_{15}^{(2\omega)} \approx 45 \times 10^{-12}$ m/V. The largest Pockels coefficient was obtained for the ACQW system with parameters $d_1 = 20$ Å, $d_2 = 16$ Å, $t_b = 5$ Å. The value of $n_3 r_{13}^{\omega} \approx 4 \times 10^{-10}$ m/V. As expected from (39) and (40) the SHG coefficient increases far more significantly with an increase in band offsets than the Pockels coefficient.

This and similar calculations for other imaginary heterostructures show that the values of nonlinear coefficients for heterostructures with large discontinuities become larger than for any known bulk inorganic materials. The fact that $\chi^{(2)}$ of the ACQW approaches $\chi^{(2)}$ of nonlinear organic materials reflects the similarity of the charge transfer process in both systems. In a nonlinear organic molecule virtual absorption of a photon causes an electron transfer from one end of the rather long molecule to the other. The distance traveled by an electron is large on atomic scale, of the order of 10 Å; hence nonlinear susceptibility is also very large. In the asymmetrical QW structure, virtual absorption of a photon causes virtual electron transfer from the confined state in the valence band to the confined state in the conduction band. The difference in dipole momentums of ground and excited states due to both asymmetry of the wells and effective mass difference is also of the order 10 Å, and that is the cause of large nonlinearity.

The major difference between QW structures and organic molecules is, as shown in the preceding section, the presence of more than one ground state in QW structures. The symmetries of these states are different and there is compensation of nonlinear polarizabilities created by transitions originating at different ground states. As a result, nonlinearity becomes resonant [hence, strong dependence of $\chi^{(2)}$ on detuning δ in (27), (28), (34), and (35)], so just like in organic materials, the major criterion of material applicability becomes whether large nonlinearity can be achieved without having large absorption.

To take full account of absorption one has to consider all the states in the bands, or to use a Kramers-Kronig approach. Still, just to estimate the order of magnitude of the ratio of $\chi^{(2)}$ to absorption, one may use the fact that energy splits $\hbar\omega_{e1}^{e2}$ and $\hbar\omega_{\mathrm{hh1}}^{\mathrm{hh2}}$, as well as detuning δ, are all larger than broadening Γ, so only the states with energies between first and second bound states in each band contribute to absorption.

In the presence of absorption there are two competing processes occurring at frequency 2ω: absorption and SHG. Under the assumptions that a fundamental wave is not depleted by SHG and the phase-matching condition is satisfied, one can write the following equations for slow electric field amplitudes $\mathbf{E}^{\omega}$ and $\mathbf{E}^{2\omega}$:

$$\frac{\partial \mathbf{E}^{2\omega}}{\partial y} = -(k/2n)[\chi^{(1)\prime\prime}(2\omega)\mathbf{E}^{2\omega} - i\chi^{(2)}(2\omega)(\mathbf{E}^{\omega})^2] , \tag{41}$$

where

$$\chi^{(1)\prime\prime}(2\omega) \approx \mathrm{Im}\left[\frac{N_z e^3 r_{e,\mathrm{hh}}^2}{3\epsilon_0 \hbar} \sum_{k_{\parallel}} \frac{\langle \psi_{\mathrm{hh1}} | \psi_{e1} \rangle^2}{\omega_{\mathrm{hh1}}^{e1}(k_{\parallel}) - 2\omega + i\Gamma}\right] \tag{42}$$

is imaginary part of linear susceptibility at frequency 2ω.

The solution of (41) is

$$\mathbf{E}^{2\omega} = i\frac{\chi^{(2)}(2\omega)(\mathbf{E}^{\omega})^2}{\chi^{(1)\prime\prime}(2\omega)}\left[1 - \exp\left[-\frac{k}{2n}\chi^{(1)\prime\prime}(2\omega)y\right]\right] . \tag{43}$$

Second-harmonic power seems to saturate at few absorption distances; therefore the maximum efficiency of SHG is

$$\eta = \frac{I^{2\omega}}{I^{\omega}} = \left[\frac{2\chi^{(2)}(2\omega)}{\chi^{(1)\prime\prime}(2\omega)}\right]^2 \frac{I^{\omega}}{c\epsilon_0} \approx \left[\frac{\langle \psi_{e2} | \psi_{\mathrm{hh1}} \rangle}{\langle \psi_{e1} | \psi_{\mathrm{hh1}} \rangle} \frac{e\langle \psi_{e1} | z | \psi_{e2} \rangle \hbar\omega_{e1}^{e2}}{(E_g - \hbar\omega)^2} \frac{\delta + \hbar\omega_{e1}^{e2}}{\Gamma}\right]^2 \frac{I^{\omega}}{cn\epsilon_0} , \tag{44}$$

where all of the assumptions about absorption made above were used. The result of (44) is very interesting from the point of view of η dependence on well thickness: On one hand, dipole momentum in the first set of large parentheses is proportional to d; on the other hand, the level splitting $\hbar\omega_{e1}^{e2}$ sharply decreases with increase in d. Larger splitting should also allow larger detuning δ further decreasing absorption. In order to make order of magnitude estimation of η, we assume

$$E_g = \approx 1.4 \text{ eV}, \quad \hbar\omega \approx 0.6 \text{ eV}, \quad d \approx 50 \text{ Å} ,$$

$$\hbar\omega_{e1}^{e2} \approx 200 \text{ meV}, \quad \delta \approx 75 \text{ meV}, \quad \Gamma \approx 25 \text{ meV} .$$

We also assume that $D_{15}^{(2\omega)}(\delta)$ has been optimized, so $\langle \psi_{e2} | \psi_{\mathrm{hh1}} \rangle \approx 0.5$, and $\langle \psi_{e1} | z | \psi_{e2} \rangle \approx d/2$. Then one obtains

$$\eta = (1.9 \times 10^{-10}) I^{\omega} , \tag{45}$$

where I^{ω} is measured in W/cm^2. Therefore, to achieve 1% conversion efficiency, the required fundamental power density is of the order of 50 MW/cm^2, about an order of magnitude higher than maximum power available from today's injection lasers. In order to increase conversion efficiency one can cool the system, thus reducing Γ, or increase simultaneously the detuning δ and the

interaction length. Still, by far the best way to improve saturation conversion efficiency is to seek novel materials with larger band offsets. Calculations for the described above the hypothetical GaAs-ZnSe MQW heterostructure show that only 2 MW/cm^2 of fundamental power is required for 1% efficient SHG conversion at a length of about 1 mm.

For linear electrooptic effect, the influence of absorption can be dealt with in a similar way. The absorption coefficient for the waveguide of one-half wavelength is

$$\alpha l^{(\lambda/2)}=\frac{2\pi\chi''^{(1)}(\omega)}{\chi^{(2)}(\omega)E_z^0}\approx\left[\frac{\langle\psi_{e2}|\psi_{hh1}\rangle}{\langle\psi_{e1}|\psi_{hh1}\rangle}\frac{e\langle\psi_{e1}|z|\psi_{e2}\rangle E_z^0}{\delta}\frac{\delta+\hbar\omega_{e1}^{e2}}{\Gamma}\right]^{-1}, \tag{46}$$

where E_z^0 is the low-frequency field applied to the system in the z direction. For the optimal GaAs-Al$_x$Ga$_{1-x}$As system described above, and $E_z^0=10^5$ V/cm, $\alpha l^{(\lambda/2)}\approx 1.2$, meaning that light is attenuated approximately three times. The absorption, in fact, is significantly larger because of the shift of the absorption due to linear confined Stark effect.

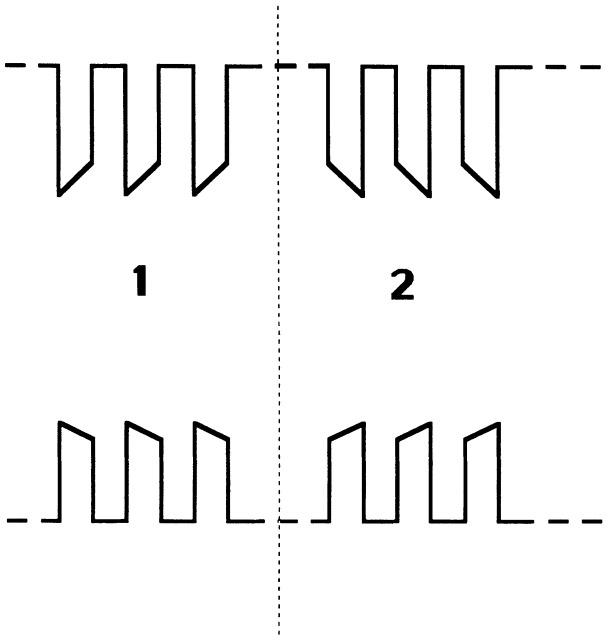

FIG. 6. Large-scale-twinned multiple quantum well structure.

V. SOME PRACTICAL APPLICATION ASPECTS

Second-order optical nonlinearity, besides being, in general, of stronger effect than third-order nonlinearity and thus being observable at lower light intensities, has another important advantage. This advantage lies in the fact, that unlike $\chi^{(3)}$, $\chi^{(2)}$ has a sign, and that sign can be easily reversed by growing the structures that are mirror images of each other (Fig. 6). One can achieve reversal of $\chi^{(2)}$ in both the ACQW and GBQW as well as in the BQW where bias is achieved by modulation doping or built-in stress. The regions in QW structures where $\chi^{(2)}$ keeps its sign are large-scale equivalents of ferroelectric domains or twins. One may call them "large-scale twins" and the whole structure in Fig. 6 "large-scale-twinned QW structure" or LSTQWS.

Without going into details, we would like to note a few useful applications of the LSTQWS. When an electric field is applied in z direction the indices of refraction in domain 1 increase and in domain 2 decrease (or vice versa). As a result, if the domain thickness is $\lambda/4$, then for light propagating in the z direction the transmission or reflectivity changes. Such a device can be a very efficient spatial modulator.

One can fabricate a waveguide around LSTQWS or, what is even better, two coupled waveguides—one around each domain. Then, a small electric field applied in the z direction shall cause the guided light to move in the z direction toward the domain with the larger n or to couple from one waveguide to another. That would create a very nice coupler or modulator. Also, such a device, being very responsive to small electric field variations, may be used in fiber-optics sensors of voltage, stress, and other parameters.

The LSTQWS is also very useful for phase matching in SHG. It is well known that in waveguides it is possible to compensate material dispersion with modal dispersion of the guide, i.e., to match phase velocities of lower-order fundamental waves, say TM$_0^\omega$ and Te$_0^\omega$ and a higher-order harmonic wave, say TM$_1^{2\omega}$. Unfortunately, the efficiency of SHG is proportional to overlap of two waves in the xz plane,

$$\eta\sim\left|\int d_{xzx}(z)E_x^{2\omega}(z)E_z^{\omega}(z)E_x^{\omega}(z)dz\right|^2, \tag{47}$$

which is very small due to the oscillatory character of $E_x^{2\omega}$. One can, however compensate for the change of sign in the electric field of the harmonic wave using the change of sign in SHG coefficient,[28] which is of course easily accomplished in the LSTQWS with two domains.

VI. CONCLUSIONS

In this work the expression for the second-order susceptibility of asymmetric QW structures based on interband transitions has been rigorously derived. It is shown that nonzero $\chi^{(2)}$ is the result of both asymmetry of band offsets and difference in effective masses of valence and conduction bands. The total $\chi^{(2)}$ is the sum of nonlinear susceptibilities arising from transitions originating from many individual electron and hole levels, and is, therefore, a much more complex function of frequency and QW parameters than intraband $\chi^{(2)}$ studied in previous works. The large number of ground and excited levels with different charge distributions results in extensive compensation. In accordance with sum rules for oscillator strength, we have shown that large separation between sublevels in each band, and therefore large band offsets, is the foremost condition necessary for large $\chi^{(2)}$.

Using the above results, in resonant approximation, ex-

pressions for SHG and Pockels coefficients were obtained. They were studied for different well geometries and materials. In GaAs-$Al_xGa_{1-x}As$ structures the magnitude of SHG and Pockels coefficients are of the order of most electrooptic materials used today. However, the room-temperature excitonic effects were not included in our calculations. According to Ref. 2 one should expect an increase in nonlinearity by an order of magnitude. We have also concluded that due to the resonance character of nonlinear effects, the practical limitation to efficiency of nonlinear or electrooptic QW devices is absorption rather than magnitude of $\chi^{(2)}$. We have also shown that the ratio of $\chi^{(2)}$ to absorption can be improved drastically by using novel heterostructures with large band offsets. For one of the hypothetical, but not entirely impractical, ZnSe-GaAs lattice-matched QW structures, our calculations predicted more than 1% SH conversion efficiency in the waveguide of only 1 mm in length.

The way toward synthesizing materials with extraordinary nonlinear properties thus lies in the direction of growing of ordered structures of two quite dissimilar materials. Obviously, one could arrive at such a conclusion without all the involved calculations performed by us, but it seems that our results based on a simple effective mass model are useful in the predictions of the magnitude of the nonlinear effects, without going into the calculation of the band structure of the new materials. Still, when band offsets and effective mass differences become large and well thicknesses small, one has to refine the theory and use a better model which would include unconfined levels and excitonic effects.

As for practical applications, we have suggested a novel type of heterostructure—LSTQWS—which has interesting electrooptics properties and allows effective phase matching. The future work should concentrate in the expanding the range of these novel materials toward visible light using II-VI semiconductors,[29] and maybe even chlorides. On the other hand, for longer-wavelength applications one should pay more attention to nonlinear devices based on intersubband transitions within the conduction band because $\chi^{(2)}$ compensation in such structures is less severe. Although not an easy way, this material engineering may become an alternative to "molecular engineering" of nonlinear organic materials and lead to further advances in integrated optoelectronics.

---

*Present address: Department of Electrical and Computer Engineering, The Johns Hopkins University, Baltimore, MD 21218.

[1]D. A. B. Miller, J. S. Weiner, and D. S. Chemla, IEEE J. Quantum Electron. **QE-22**, 1816 (1986).
[2]Y.-C. Chang, J. Appl. Phys. **58**, 499 (1985).
[3]W. L. Bloss and L. Friedman, Appl. Phys. Lett. **41**, 1023 (1982).
[4]C. Cooperman, L. Friedman, and W. L. Bloss, Appl. Phys. Lett. **44**, 977 (1982).
[5]D. S. Chemla and D. A. B. Miller, J. Opt. Soc. Am. B **2**, 1155 (1985).
[6]D. S. Chemla, T. C. Damen, D. A. B. Miller, A. C. Gossard, and W. Wiegmann, Appl. Phys. Lett. **44**, 16 (1984).
[7]T. H. Wood, R. W. Tkach, and A. R. Chapllyvy, Appl. Phys. Lett. **50**, 798 (1987).
[8]D. A. B. Miller, D. S. Chemla, T. C. Damen, A. C. Gossard, W. Wiegmann, T. H. Wood, and C. A. Burrus, Appl. Phys. Lett. **45**, 13 (1984).
[9]C. Flytzanis, in *Nonlinear Optics,* Vol. I of *Quantum Electronics,* edited by H. Rabin and C. L. Tang (Academic, New York, 1975), Pt. A, pp. 18–22.
[10]T. Taniuchi, K. Yamamoto, in Digest of 1987 Conference on Lasers and Electro-Optics (CLEO '87), Baltimore, MD, 1987, p. 198 (unpublished).
[11]G. C. Osbourn, IEEE J. Quantum Electron. **QE-22**, 1677 (1986).
[12]G. H. Dohler, IEEE J. Quantum Electron. **QE-22**, 1682 (1986).
[13]C. Flytzanis and J. Ducuing, Phys. Rev. **178**, 1218 (1976).
[14]M. K. Gurnick and T. A. De Temple, IEEE J. Quantum Electron. **QE-19**, 791 (1983).
[15]B. F. Levine, R. J. Malik, J. Walter, K. K. Choi, C. G. Bethea, D. A. Kleinman, and J. M. Vandenberg, Appl. Phys. Lett. **50**, 273 (1987).
[16]R. Tsu and L. Esaki, Appl. Phys. Lett. **19**, 246 (1971).
[17]H. Q. Le, J. J. Zayhowski, and W. D. Goodhue, Appl. Phys. Lett. **50**, 1518 (1987).
[18]J. W. Little, J. K. Whisnant, R. P. Levitt, and R. A. Wilson, Appl. Phys. Lett. **51**, 1786 (1987).
[19]K. Nishi and T. Hiroshima, Appl. Phys. Lett. **51**, 320 (1987).
[20]M. Yamanishi, Phys. Rev. Lett. **59**, 1014 (1987).
[21]D. S. Chemla, D. A. B. Miller, and S. Shmitt-Rank, Phys. Rev. Lett. **59**, 1018 (1987).
[22]J. Khurgin, Appl. Phys. Lett. **51**, 2100 (1987).
[23]E. O. Kane, J. Phys. Chem. Solids **1**, 249 (1957).
[24]N. Bloembergen, *Nonlinear Optics* (Benjamin, New York, 1965).
[25]G. Bastard and J. A. Brum, IEEE J. Quantum Electron. **QE-22**, 1625 (1986).
[26]D. R. Penn, Phys. Rev. **12**, 2093 (1962).
[27]S. P. Kowalczyk, E. A. Kraut, J. R. Waldrop, and R. W. Grant, J. Vac. Sci. Technol. **21**, 482 (1982).
[28]N. Bloembergen, U.S. Patent No. 3 384 433 (1968).
[29]L. A. Kolodziejski, R. L. Gunshor, N. Otsuka, S. Datta, W. M. Becker, and A. V. Nurmikko, IEEE J. Quantum Electron. **QE-22**, 1666 (1986).